https://doi.org/10.5194/egusphere-2026-5019
Preprint. Discussion started: 14 September 2026
© Author(s) 2026. CC BY 4.0 License.

Distribution and biogeochemical controls of dissolved cobalamin (vitamin B_{12}) in the western North Pacific

Yoshiko Kondo[1,2]*, Yukiko Kawakami[2], Tomohiro Takatani[1,2], Toshikazu Suzuki[1,2], Hajime Obata[3], Jun Nishioka[4]

[1] Graduate School of Integrated Science and Technology, Nagasaki University, Nagasaki, Japan
[2] Graduate School of Fisheries and Environmental Sciences, Nagasaki University, Nagasaki, Japan
[3] Atmosphere and Ocean Research Institute, The University of Tokyo, Japan
[4] Pan-Okhotsk Research Center, Institute of Low Temperature Science, Hokkaido University, Japan

Correspondence to: Yoshiko Kondo (yoshikondo@nagasaki-u.ac.jp)

Abstract

Vitamin B_{12} (cobalamin) is an essential micronutrient for many marine microorganisms, yet its distribution and biogeochemical controls in the open ocean, particularly below the euphotic zone, remain poorly constrained. We investigated the vertical and zonal distributions of four dissolved cobalamin species from the surface to the deep western North Pacific. Total dissolved cobalamin (TD-B_{12}) concentrations ranged from below detection to 1.63 pM and were generally low in surface waters. Elevated concentrations occurred below the subsurface chlorophyll maximum (SCM), extended into the upper North Pacific Intermediate Water (NPIW) at northern stations, and were also observed locally in bottom waters. Hydroxocobalamin (OH-B_{12}) was the dominant dissolved form throughout most of the water column. From the surface to the upper NPIW, TD-B_{12} increased with apparent oxygen utilization (AOU), consistent with a contribution of organic matter remineralization to cobalamin accumulation. TD-B_{12} was also positively associated with the relative abundance of Nitrosopumiliaceae inferred from 16S rRNA gene amplicon sequencing, indicating an association between cobalamin accumulation and microbial community composition. In contrast, the relationship between TD-B_{12} and AOU disappeared below the lower NPIW, suggesting that remineralization alone cannot explain cobalamin distributions at greater depths. Elevated cobalamin within the upper NPIW suggests a role for intermediate-water transport, whereas localized bottom-water enrichment may reflect benthic sources and deep-water circulation. Overall, dissolved cobalamin distributions reflect a depth-dependent balance among microbial cycling, degradation, and physical transport.

1 Introduction

Vitamin B_{12} (cobalamin) is an essential cobalt-containing micronutrient required by approximately half of marine eukaryotic phytoplankton for key metabolic pathways, including methionine synthesis and ribonucleotide reduction (Sañudo-Wilhelmy et al., 2014). Because only a limited group of bacteria and archaea can synthesize cobalamin de novo, the availability

https://doi.org/10.5194/egusphere-2026-5019
Preprint. Discussion started: 14 September 2026
© Author(s) 2026. CC BY 4.0 License.

of dissolved cobalamin in seawater depends on complex interactions among microbial production, biological consumption, and physicochemical transformation (Croft et al. 2005; Sañudo-Wilhelmy et al. 2014). Consequently, cobalamin has been recognized as an important micronutrient influencing marine primary productivity, microbial interactions, and biogeochemical cycling (Bertrand et al., 2007; Sañudo-Wilhelmy et al., 2012).

Recent advances in liquid chromatography–mass spectrometry (LC–MS) have enabled simultaneous determination of multiple dissolved cobalamin species in seawater, allowing their distributions to be investigated in various marine environments (Heal et al., 2014; Suffridge et al., 2018; Bannon et al., 2025). Although early bioassay-based studies reported vertical distributions of cobalamin extending into the deep ocean (Daisley and Fisher, 1958; Menzel and Spaeth, 1962; Carlucci and Cuhel, 1977), depth-resolved observations of multiple cobalamin species from the surface to the deep ocean remain scarce. The relative importance of the biogeochemical processes controlling dissolved cobalamin distributions, including microbial production, biological uptake, photochemical degradation, remineralization of sinking organic matter, and physical transport by ocean circulation remains poorly understood (Bertrand et al., accepted). Disentangling the relative contributions of these processes is essential for understanding the role of cobalamin in marine biogeochemical cycles and its availability to marine microorganisms.

The western North Pacific is one of the most biogeochemically dynamic regions of the global ocean. Strong meridional gradients in nutrient availability, active intermediate-water formation, and vigorous circulation connect productive marginal seas with the open North Pacific through North Pacific Intermediate Water (NPIW) (Nishioka et al., 2020). This region therefore provides an excellent natural laboratory for investigating how biological processes and water-mass transport together regulate the distribution of dissolved micronutrients. Although iron and macronutrient cycling have been extensively investigated in this region (Nishioka et al., 2021), basin-scale observations of dissolved cobalamin remain scarce, particularly below the euphotic zone where regeneration and intermediate water transport may strongly influence its distribution.

In this study, we determined the vertical distributions of four dissolved cobalamin species (cyanocobalamin (CN-B_{12}), hydroxocobalamin (OH-B_{12}), methylcobalamin (CH_3-B_{12}), and adenosylcobalamin (Ado-B_{12})) from the surface to the deep western North Pacific. By integrating cobalamin speciation with hydrographic observations and microbial community data, we sought to identify the major biogeochemical processes controlling dissolved cobalamin distributions, with particular emphasis on regeneration in subsurface and intermediate waters and transport by ocean circulation. These observations provide a new observational framework for understanding the marine cobalamin cycle in the western North Pacific.

2 Methods

2.1 Sample collection

Seawater samples were obtained from six stations in the equatorial and mid-latitude regions of the western Pacific onboard the *R/V* Hakuho maru KH-22-7 (GEOTRACES GP22) cruise between June 30 and September 1, 2022 (Fig. 2).

https://doi.org/10.5194/egusphere-2026-5019
Preprint. Discussion started: 14 September 2026
© Author(s) 2026. CC BY 4.0 License.

Samples were collected using acid-cleaned Teflon-coated 12-L Niskin-X bottles attached to a CTD-carousel sampling system (Seabird Electronics, Model SBE-9-plus, SBE-3, SBE-4 and SEB 43).

The seawater samples for the analysis of dissolved cobalamin were filtered through an acid-cleaned AcroPak 200 Capsule filter with a 0.2 μm-pore-size Supor Membrane (Pall) and collected in 2 L amber high-density polyethylene bottles (Nalgene). The pH of the filtered sample was adjusted to 6–6.5 using diluted hydrochloric acid (Fujifilm Wako Pure Chemical). The water samples were preconcentrated to measure four types of cobalamin (CN-B_{12}, OH-B_{12}, CH_3-B_{12}, and Ado-B_{12}) using solid-phase extraction with a C_{18} resin (HF Bodesil C_{18}, Agilent), followed by elution with 10 mL methanol (LC-MS grade, Fujifilm-Wako Chemical) (Sañudo-Wilhelmy et al., 2012; Suffridge et al., 2017). Both pH adjustment and extraction into methanol were carried out in a dark room, then the extract was kept in -20°C freezer and brought back to the onshore laboratory.

Seawater samples (1 L) for prokaryotic community analysis were immediately filtered through Steribex filters (pore size: 0.2 μm), and the filter samples were stored below -20 °C until analysis. The seawater samples were also collected from the upper 200 m for the determination of chlorophyll *a* concentration and immediately filtered through GF/F filters (Whatman). Chlorophyll *a* was extracted from 6-mL aliquots of N,N-dimethylformamide, stored at -20 °C for over 24 h. At the subsurface chlorophyll maximum layer, seawater samples for determining phytoplankton composition were obtained and fixed with acidic Lugol's solution (final concentration: 2%).

https://doi.org/10.5194/egusphere-2026-5019
Preprint. Discussion started: 14 September 2026
© Author(s) 2026. CC BY 4.0 License.

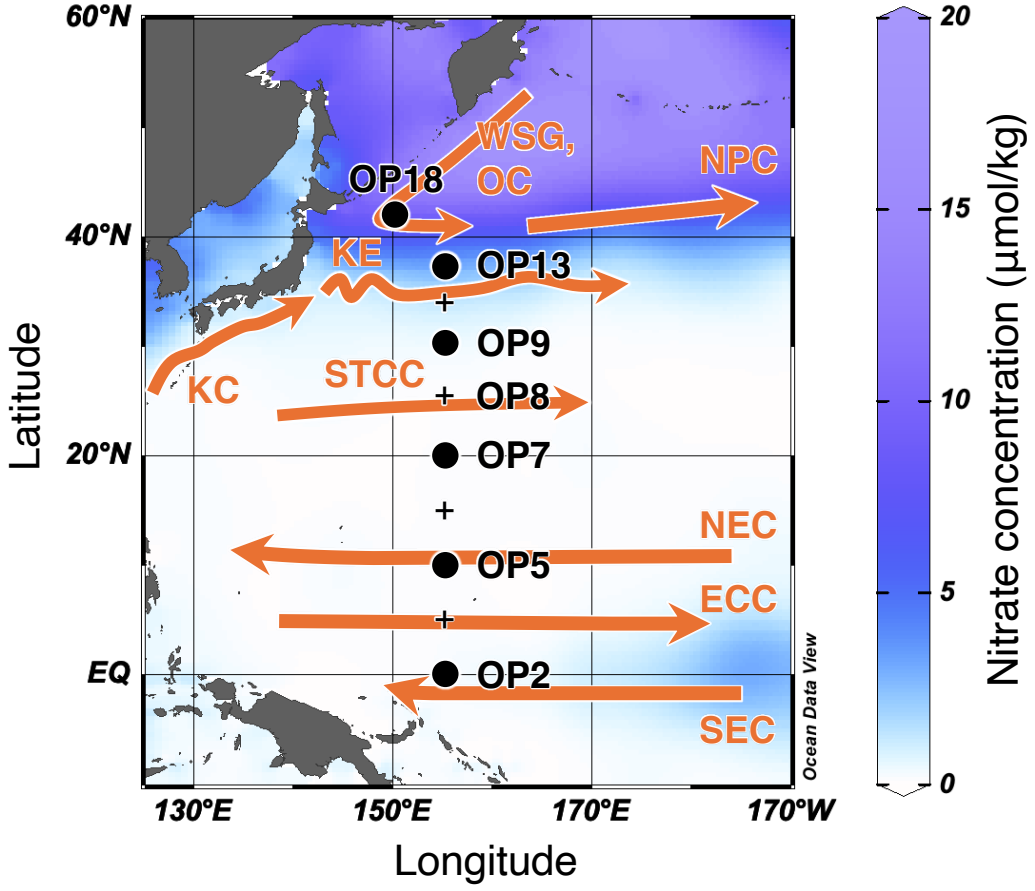

Figure 1: Sampling locations (black filled circles) during *R/V* Hakuho maru KH-22-7 cruise. Cross symbols indicate locations where only the hydrographic parameters were obtained. The background color shows the surface nitrate concentrations obtained from the World Ocean Atlas (2018). The bold arrows indicate the surface water current directions in this region (WSG: Western Subarctic Gyre, OC: Oyashio, KC: Kuroshio, KE: Kuroshio Extension, STCC: Subtropical Counter Current, NPC: North Pacific Current, NEC: North Equatorial Current, ECC: Equatorial Counter Current, SEC: South Equatorial Current) (Talley et al., 2011).

2.2 Cobalamin analysis

The methanol extracts were evaporated under a stream of nitrogen and concentrated by a factor of approximately 8000 prior to analysis. The analysis of dissolved cobalamin samples was conducted using ultra-high-performance liquid chromatography–mass spectrometry (UPLC-MS; ACQUITY UPLC I-Class PLUS Module-Quattro micro API, Waters) with a reversed-phase column (ACQUITY UPLC HSS Cyano 1.8-µm 2.1×100-mm column, Waters). An 8.31-min gradient flow

https://doi.org/10.5194/egusphere-2026-5019
Preprint. Discussion started: 14 September 2026
© Author(s) 2026. CC BY 4.0 License.

was used with mobile phases (mobile A: 0.1% formic acid and 1 M ammonium formate (LC-MS grade, Fujifilm-Wako Pure Chemical) and mobile B: 100% acetonitrile (LC-MS grade, Fisher Scientific) (Table 1). The mass spectrometer was run in the multiple reaction mode (MRM) with positive polarity. The ESI spray source temperature, desolvation temperature, cone gas flow, desolvation gas flow, capillary voltage, and sample flow rate were 130 °C, 450 °C, 55 L/h, 550 L/h, 2000 V, and 0.35 mL/min, respectively. The m/z values of each cobalamin type and its respective ions, as well as the specific collision energy, cone voltage, and recovery efficiencies are listed in Table 2. In this study, no cobalamin signal was present in the analytical blanks, and analytical errors for CN-B_{12}, OH-B_{12}, CH_3-B_{12}, and Ado-B_{12} of the UPLC instrument were 1.0, 0.9, 1.0, and 0.8 nM respectively (n=5), from three times the standard deviation of the lowest detectable concentration of the mixed standard (2.5 ppb); similar values were obtained in a previous study (Suffridge et al., 2017). The procedural limits of detection depend on the preconcentration factors, which varied from 7960 to 8360 for each sample in this study. The final concentration for each cobalamin concentration was determined based on the average recovery rate shown in Table 2. We conclude that this method could detect differences in CN-B_{12}, OH-B_{12}, CH_3-B_{12}, and Ado-B_{12} concentrations between 0.12 and 0.13 pM, 0.11 and 0.12 pM, 0.12 pM, and 0.098 and 0.10 pM in a sample concentrated approximately 8000 times.

Table 1: Gradient flow for UPLC-MS used in this study. Mobile phase A: 0.1% formic acid and 1 M ammonium formate, mobile phase B: 100% acetonitrile.

Time (min)	mobile phase	
	A (%)	B (%)
0	98	2
5.3	70	30
6.3	5	95
6.31	98	2
8.31	98	2

Table 2: Analytical parameters of UPLC-MS and spike recovery for measured analytes in this study.

Analyte	MRM parent-product (m/z)	Collision energy (V)	Cone voltage (V)	Retention time (min)	Spike recovery (%) (n=3)
cyanocobalamin	678.6 - 147.1, 359.2	35	25	3.97	83.9±4.2
hydroxocobalamin	664.7 - 147.1, 359.2	33	20	3.56	59.0±11.1
methylcobalamin	673.1 - 147.1, 685.6	36	22	5.14	83.9±2.9
adenosylcobalamin	790.7 - 147.1, 665.6	40	25	4.48	92.1±4.1

https://doi.org/10.5194/egusphere-2026-5019
Preprint. Discussion started: 14 September 2026
© Author(s) 2026. CC BY 4.0 License.

2.3 Prokaryotic community composition based on 16S rRNA gene amplicon sequencing

DNA extraction and 16S rRNA data analysis of the filter samples were outsourced and obtained from the Bioengineering Institute of Japan. After adding Lysis Solution F (Nippon Gene) to the filter paper, the samples were ground and left to stand at 65 °C for 10 min. The samples were then centrifuged at 12000 × g for 1 min, and the supernatant was separated. DNA was purified using a LabAid 824 DNA Extraction Kit (ZEESAN). The concentration of the DNA solution was measured using Synergy LX (BioTek) and a QuantiFluor dsDNA System (Promega). The library was prepared using a two-step tailed PCR method with primers 515F-Y (5′-GTGYCAGCMGCCGCGGTAA) and 926R (5′-CCGYCAATTYMTTTRAGTTT) (Parada et al., 2016). The concentration of the generated libraries was measured using Synergy H1 (BioTek) and a QuantiFluor dsDNA System. The quality of the prepared libraries was confirmed using a Fragment Analyzer and dsDNA 915 Reagent Kit (Advanced Analytical Technologies). Sequencing was performed using the MiSeq system and the MiSeq Reagent Kit v 3 (Illumina) at 2 × 300 bp.

The FASTX Toolkit (version 0.0.14) was used to extract reads that matched the primer sequences. Only the read sequences whose beginnings completely matched the primer sequences used were extracted. Primer sequences were removed from the extracted reads using the fastx_trimer from the FASTX Toolkit. Sequences with a quality value of less than 20 were removed using sickle (version 1.33), and sequences with a length of 130 bases or less and their paired sequences were discarded. Reads were joined using the paired-end read-joining script FLASH (version 1.2. 11) with a minimum overlap of 10 bases. After removing chimeric and noise sequences using the Dada 2 plugin in Qiime2 (version 2022.8), representative sequences and an ASV table were obtained. Using the feature classifier plugin, the representative sequences were compared with 99 OTUs in Silva (version 138) to infer the phylogeny.

Relative abundances of microbial taxa were determined from 16S rRNA gene amplicon sequencing and are expressed as the proportion of sequencing reads assigned to each taxon. These values represent relative community composition rather than absolute cell abundances.

2.4 Other parameters

Chlorophyll *a* concentration was determined using a fluorometer (10-AU, Turner Design Inc.) on board (Welschmeyer, 1994). Phytoplankton cell counts were analyzed using a Sedgwick–Rafter slide and an inverted microscope (IX71, Olympus, Tokyo, Japan) (Edler and Elbrächter, 2010). The temperature, salinity, and dissolved oxygen were obtained from the CTD sensors (Seabird Electronics, Model SBE-9-plus, SBE-3, SBE-4 and SEB 43). The apparent oxygen utilization (AOU) was calculated from dissolved oxygen, temperature, and salinity using the Ocean Data View program (https://odv.awi.de/).

https://doi.org/10.5194/egusphere-2026-5019
Preprint. Discussion started: 14 September 2026
© Author(s) 2026. CC BY 4.0 License.

3 Results

3.1 Hydrography of the study area

This study crosses areas influenced by several water masses and surface ocean currents, such as the Western Subarctic Gyre (WSG), Kuroshio Extension (KE), Subtropical Counter Current (STCC), North Equatorial Current (NEC), Equatorial Counter Current (ECC), and South Equatorial Current (SEC) (Fig. 1). Water temperature and salinity in the surface mixed layer varied depending on the station (Fig. 2). Station OP13 (hereafter OP13) is located in the Kuroshio–Oyashio transition area. The chlorophyll *a* concentration was relatively low in this study area (<0.5 μg/L), the depth of the subsurface chlorophyll maximum layer (SCM) ranged between 35 and 135 m, and the shallowest layer was found in the western subarctic gyre (OP18). Subtropical Mode Water (STMW) (σ_θ=25.2–25.8) (Yasuda, 2003) was distributed around 200-m depth at OP9. Below the subsurface water, the NPIW was distributed from 340 to 1500-m depth (σ_θ=26.6–27.5) north of 20°N. The NPIW density range was significantly influenced by water from the Okhotsk Sea in the upper part, which can be identified by a lower salinity water mass (Figs. 2b) (upper NPIW, σ_θ=26.6-27.0), and the East Kamchatka Current in the lower part (lower NPIW, σ_θ=27.0-27.5) (Yasuda et al., 2001). South of 20°N, the Equatorial Pacific Intermediate Water (EqPIW) is distributed below the subsurface water (salinity = 34.5-34.6, average σ_θ=27.3) (Bostock et al., 2010). In the NPIW and EqPIW, salinity varied with latitude, with lower values in the 200–1000-m layer north of 20°N, and higher values in the equatorial area. A rapid decrease in dissolved oxygen and increase in AOU were also observed below the subsurface layer. Below the NPIW or EqPIW, Pacific Deep Water (PDW) (σ_θ>27.5, σ_4<45.88) and Lower Circumpolar Deep Water (LCDW) (σ_4>45.88) were distributed up to the 4000-m layer and deeper, respectively (Talley et al., 2011). Based on the seafloor topography, the Upper Circumpolar Deep Water (UCDW) flowed into the deep layer at OP2 (Kawabe and Fujio, 2010).

https://doi.org/10.5194/egusphere-2026-5019
Preprint. Discussion started: 14 September 2026
© Author(s) 2026. CC BY 4.0 License.

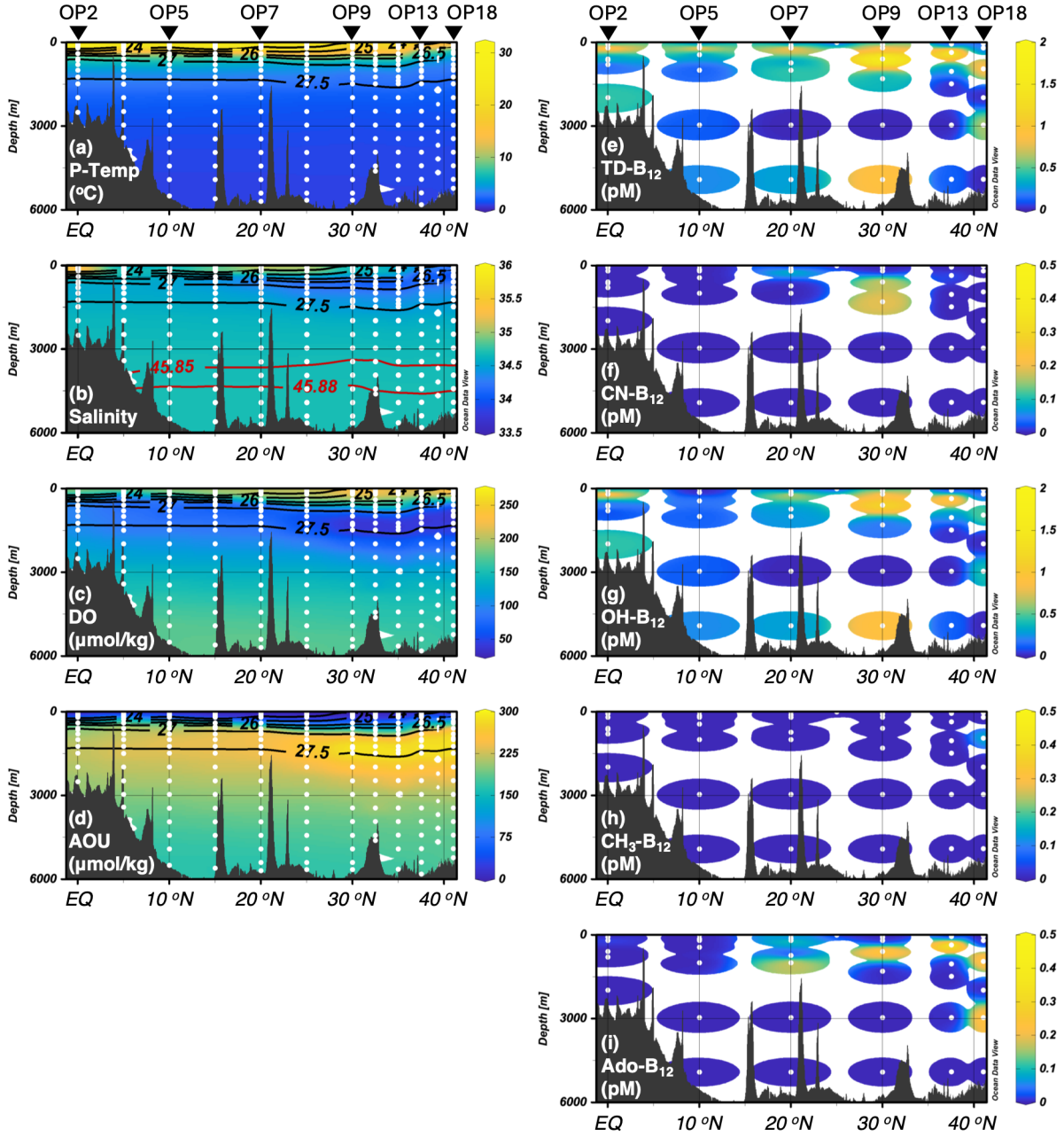

Figure 2: Vertical sections from OP2 to OP18 along 155°E and 150°E showing (a) potential temperature (P-Temp), (b) salinity, (c) dissolved oxygen (DO), (d) apparent oxygen utilization (AOU), (e) total dissolved cobalamin (TD-B_{12}), (f) cyanocobalamin (CN-B_{12}), (g) hydroxocobalamin (OH-B_{12}), (h) methylcobalamin (CH_3-B_{12}), and (i) adenosylcobalamin (Ado-B_{12}). The black lines in (a)–(d) represent the isopycnal surfaces of potential density anomalies (σ_0), and the red lines in (b) represent potential density isopycnals based on 4000 m (σ_4).

https://doi.org/10.5194/egusphere-2026-5019
Preprint. Discussion started: 14 September 2026
© Author(s) 2026. CC BY 4.0 License.

3.2 Distribution of dissolved cobalamin in the western North Pacific

The concentrations of total dissolved cobalamin (TD-B_{12}, the sum of the four types of cobalamin) and its four dissolved species (CN-B_{12}, OH-B_{12}, CH_3-B_{12}, and Ado-B_{12}) exhibited distinct vertical and latitudinal variations throughout the western North Pacific (Figs. 2 and 3). TD-B_{12} concentrations ranged from below the detection limit to 1.63 pM across this study area. Surface TD-B_{12} concentrations were generally low at most stations. Elevated concentrations were consistently observed below the SCM, typically at approximately 200 m depth, and frequently extended into the upper NPIW at stations north of 20ºN. In addition, relatively high TD-B_{12} concentrations were found in bottom waters (approximately 5000 m depth) at several stations, although regional differences were apparent among water masses.

OH-B_{12} was the dominant dissolved cobalamin species throughout the water column, including near bottom waters, and accounted for the largest proportion of TD-B_{12} at nearly all stations; OH-B_{12} accounted for 37% to 100% of the TD-B_{12} below the SCM, within the upper NPIW, and it constituted 100% in the bottom water. In contrast, CN-B_{12} was detected only sporadically, with a maximum concentration of 0.24 pM. Similarly, CH_3-B_{12} was detected only at the northernmost station, where the concentration was 0.14 pM. In contrast, Ado-B_{12} tended to exhibit elevated concentrations in the upper intermediate waters north of 20ºN. Latitudinal differences were also evident; stations in the subarctic region generally exhibited higher TD-B_{12} concentrations than those in the subtropical region, particularly in the intermediate waters. Elevated concentrations of OH-B_{12} and Ado-B_{12} largely accounted for this difference, whereas the distributions of CN-B_{12} and CH_3-B_{12} showed comparatively small regional variations. Ado-B_{12} contributed a larger fraction in the samples with high TD-B_{12} samples, including those from the upper intermediate waters, whereas CH_3-B_{12} represented only a minor fraction throughout the water column.

https://doi.org/10.5194/egusphere-2026-5019
Preprint. Discussion started: 14 September 2026
© Author(s) 2026. CC BY 4.0 License.

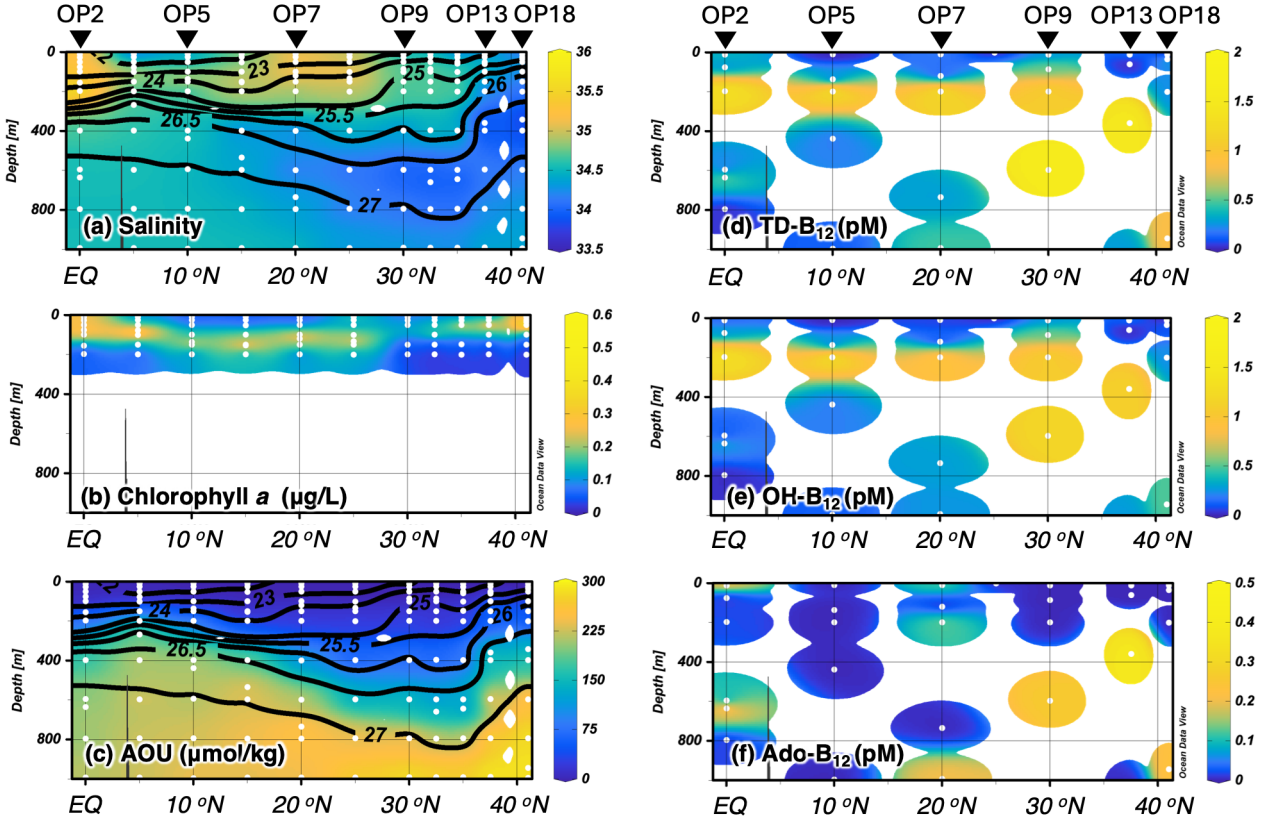

Figure 3: Upper 1000-m vertical sections from OP2 to OP18 along 155°E and 150°E for (a) salinity, (b) chlorophyll *a*, (c) AOU, (d) TD-B$_{12}$, (e) OH-B$_{12}$, and (f) Ado-B$_{12}$. The isopycnals in (a) and (c) represent potential density anomalies (σ_θ).

3.3. Phytoplankton and prokaryotic community composition

Chlorophyll *a* concentrations were generally low throughout the study area, with values below 1 μg/L at all stations (Fig. 3). A SCM was observed at most stations, although chlorophyll *a* concentrations remained relatively low compared with those typically observed in more productive regions. Microscopic observations of phytoplankton were conducted only for samples collected from the SCM layer (Fig. 4). Phytoplankton community composition varied among stations, with differences in the relative contributions of major taxonomic groups. The composition of prokaryotic communities exhibited clear vertical variation (Fig. 5). The relative abundance of Nitrosopumiliaceae was low in surface waters but increased below the SCM and remained relatively high within the upper intermediate waters. Other major bacterial groups showed distinct depth-dependent distributions, reflecting changes in microbial community composition with depth.

https://doi.org/10.5194/egusphere-2026-5019
Preprint. Discussion started: 14 September 2026
© Author(s) 2026. CC BY 4.0 License.

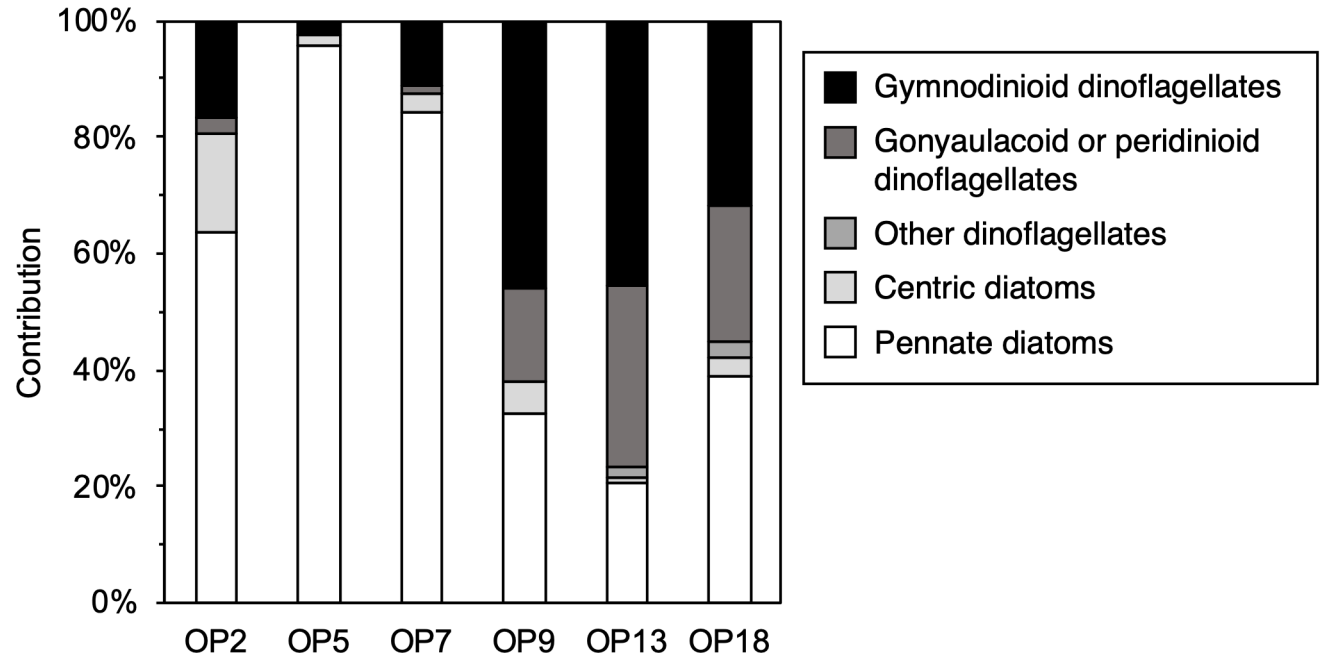

205 **Figure 4: Phytoplankton composition in the SCM layer at each station estimated from cell density observed by optical microscopy.**

https://doi.org/10.5194/egusphere-2026-5019
Preprint. Discussion started: 14 September 2026
© Author(s) 2026. CC BY 4.0 License.

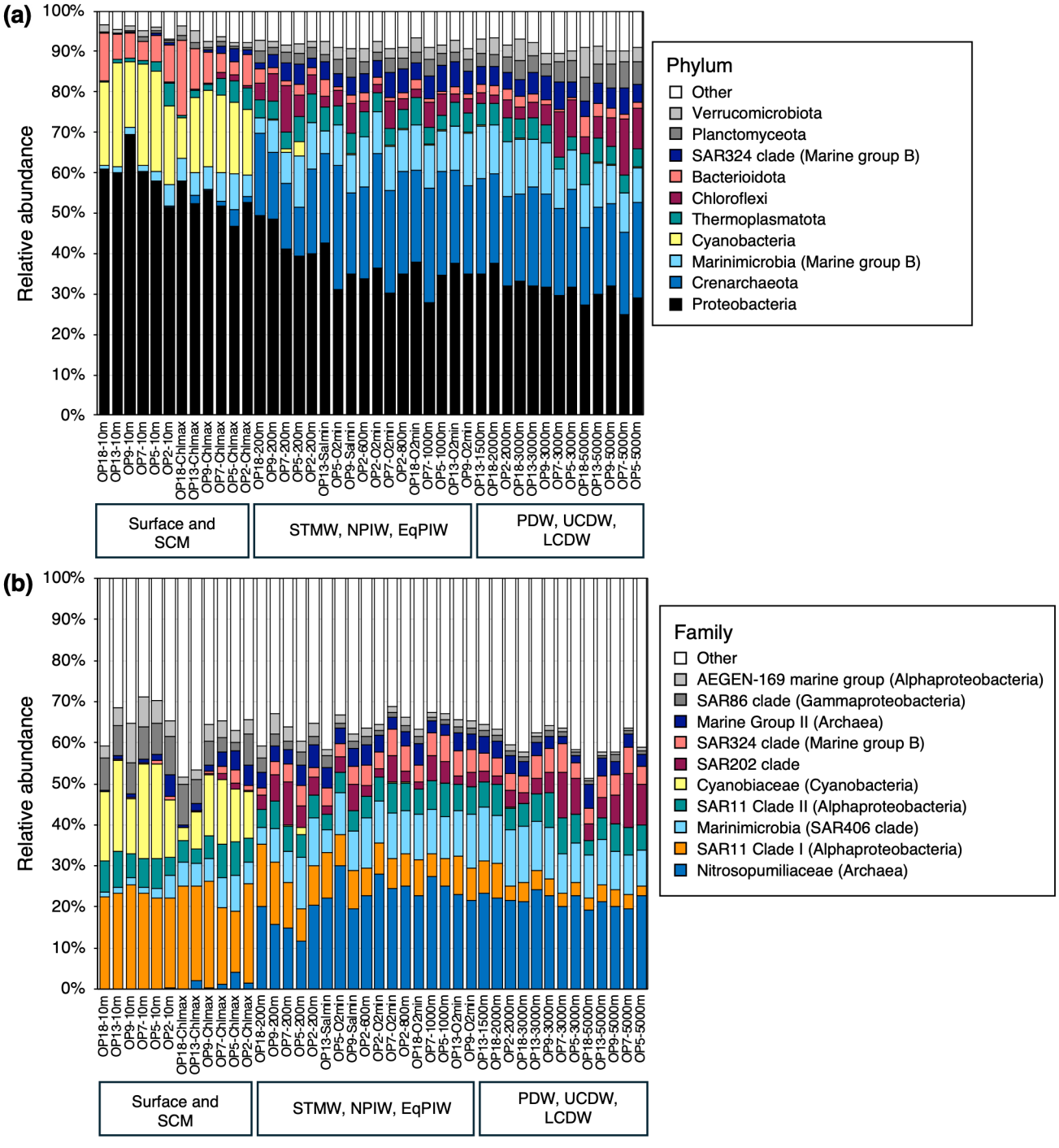

Figure 5: Relative abundance of prokaryotes at phylum and family levels in this study according to 16S rRNA gene amplicon data analysis. Abundance at the (a) phylum and (b) family levels. Prokaryotic taxa below the top-ten most abundant groups are summarized as "Other."

https://doi.org/10.5194/egusphere-2026-5019
Preprint. Discussion started: 14 September 2026
© Author(s) 2026. CC BY 4.0 License.

3.4. Relationships between dissolved cobalamin species and environmental variables

Relationships between dissolved cobalamin concentrations and AOU differed among depth ranges and cobalamin species (Fig. 6 (a)-(c)). From the surface to the upper NPIW, TD-B_{12} was positively correlated with AOU (Pearson's $r = 0.55$, $p = 0.012$), with OH-B_{12} exhibiting a similar relationship ($r = 0.54$, $p = 0.013$). In contrast, Ado-B_{12} showed no significant relationship with AOU ($r = 0.36$, $p = 0.115$). These relationships between TD-B_{12} or OH-B_{12} and AOU, however, appeared to be partly driven by the contrast between surface samples characterized by both low AOU and low cobalamin concentrations and deeper samples with higher AOU and cobalamin concentrations, rather than by a uniform relationship across the entire depth range. In the lower NPIW and deeper waters, no clear relationship between AOU and dissolved cobalamin was observed, with AOU remaining relatively high while cobalamin concentrations were variable.

Dissolved cobalamin concentrations were also compared with the relative abundance of major prokaryotic groups determined by 16S rRNA gene amplicon sequencing (Fig. 6 (d)-(f)). TD-B_{12} and OH-B_{12} showed positive relationships with the relative abundance of Nitrosopumiliaceae from the surface to the upper NPIW. In contrast, Ado-B_{12} showed no clear relationship with Nitrosopumiliaceae. Because the sequencing data represent relative sequence abundance rather than absolute cell abundance, these relationships describe changes in microbial community composition rather than quantitative changes in microbial abundance.

https://doi.org/10.5194/egusphere-2026-5019
Preprint. Discussion started: 14 September 2026
© Author(s) 2026. CC BY 4.0 License.

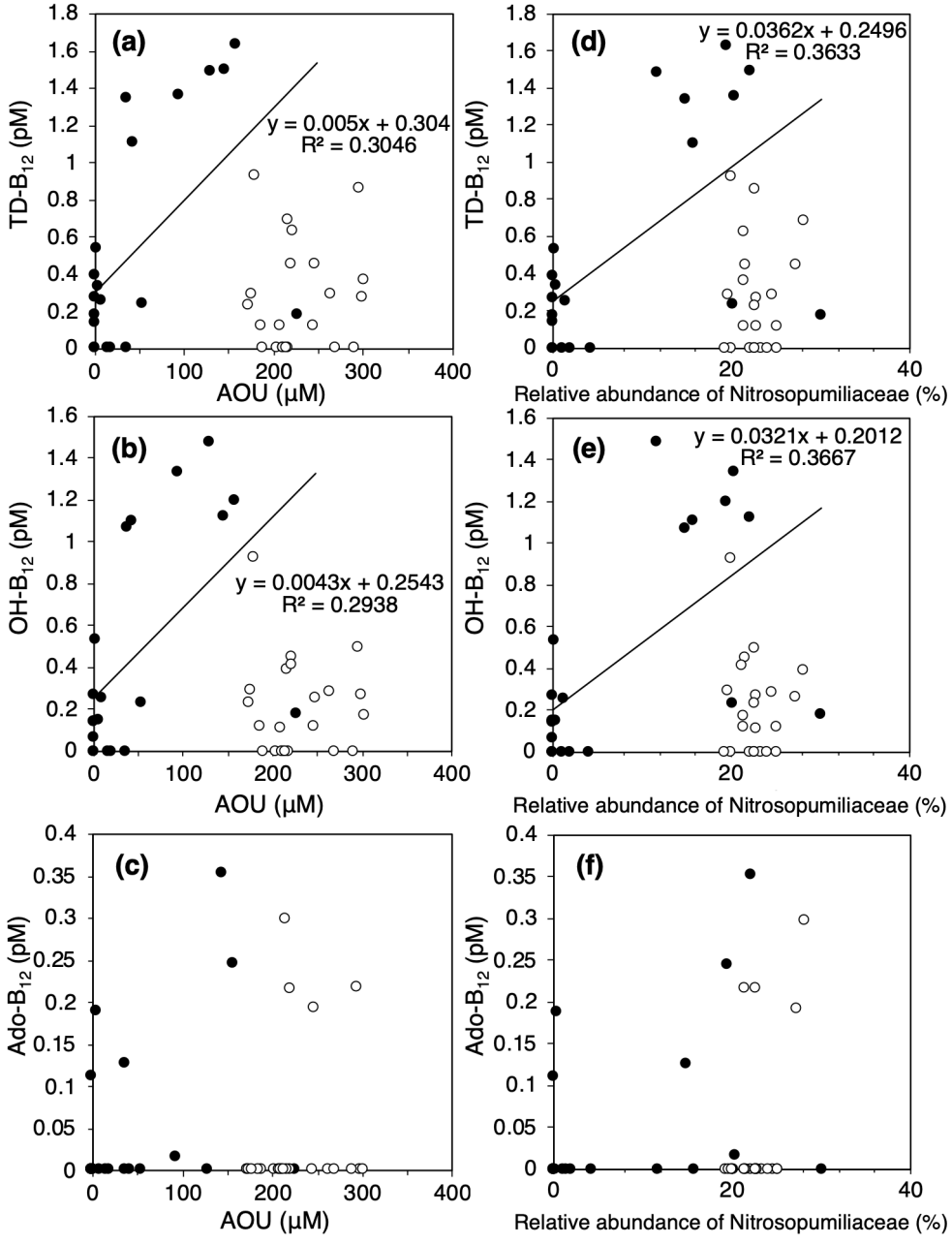

Figure 6: Relationships of dissolved cobalamin with AOU and the relative abundance of Nitrosopumiliaceae determined by 16S rRNA gene amplicon sequencing in the western North Pacific. Relationships of TD-B_{12} (a, d), OH-B_{12} (b, e), and Ado-B_{12} (c, f) with AOU (a-c) and Nitrosopumiliaceae (d-f) are shown. Closed and open circles indicate the samples from the surface to the upper NPIW and from the lower NPIW and deeper waters, respectively. Solid lines indicate linear regressions for samples from the surface to the upper NPIW.

https://doi.org/10.5194/egusphere-2026-5019
Preprint. Discussion started: 14 September 2026
© Author(s) 2026. CC BY 4.0 License.

4. Discussion

4.1 Controls on dissolved cobalamin distributions

Dissolved cobalamin exhibited pronounced vertical variations across the western North Pacific, with generally low concentrations in surface waters and elevated concentrations below the SCM and into the upper NPIW. Among the four cobalamin species examined, OH-B_{12} was the dominant form throughout most of the water column and largely determined the vertical distribution of TD-B_{12}. The predominance of OH-B_{12} is consistent with previous observations in marine waters (Heal et al., 2014) and with experimental evidence showing that OH-B_{12} is relatively stable in seawater compared with the coenzyme forms Ado-B_{12} and CH_3-B_{12} (Bannon et al., 2024). Dissolved cobalamin concentrations observed in this study were within the range previously reported for open ocean (Bertrand et al., accepted). Although very few studies have investigated the distribution of dissolved cobalamin at depths greater than 2000 m in the open ocean, comparable concentrations have been reported in the Sargasso Sea (Menzel and Spaeth, 1962). In contrast, concentrations exceeding 2 pM have been observed in regions such as the Southern Ocean (Carlucci and Cuhel, 1977) and the Bay of Biscay (Daisley and Fisher, 1958). Therefore, the concentration range observed in this study area is not particularly high. A notable feature of the present dataset is the vertical pattern, characterized by low surface concentrations and accumulation below the SCM and into intermediate waters.

The low TD-B_{12} concentrations in surface waters may reflect the combined effects of biological utilization and photochemical reactions. Cobalamin auxotrophy is widespread among marine eukaryotic phytoplankton and prokaryotes (Sañudo-Wilhelmy et al., 2014), providing an important potential sink for dissolved cobalamin in the euphotic zone. Cyanobacteria were also abundant in the upper water column, although *Prochlorococcus* and *Synechococcus* primarily produce pseudocobalamin, which differs from cobalamin in its bioavailability to eukaryotic phytoplankton (Helliwell et al., 2016). In addition to biological utilization, the coenzyme forms Ado-B_{12} and CH_3-B_{12} are less stable in sunlit seawater than OH-B_{12} (Bannon et al., 2024). Biological utilization together with photochemical transformation may therefore contribute to the low dissolved cobalamin concentrations observed in surface waters.

In contrast, TD-B_{12} concentrations increased below the SCM and remained relatively high toward the upper NPIW. TD-B_{12} and OH-B_{12} showed positive relationships with AOU from the surface to the upper NPIW, whereas Ado-B_{12} showed no significant relationship with AOU. Remineralization of sinking organic matter has been proposed as a potential source of dissolved cobalamin below the euphotic zone (Karl, 2002). AOU, TD-B_{12}, and OH-B_{12} were generally low in surface waters and increased below the SCM, partly accounting for the observed positive relationships. This concurrent increase is consistent with a contribution of organic matter remineralization to cobalamin accumulation in subsurface waters. Decomposition of microbial biomass and sinking particles could release intracellular cobalamin into the dissolved pool, followed by transformation among cobalamin forms. Such transformation may partly explain the predominance of OH-B_{12}, the relatively stable form, throughout much of the water column. Recent culture experiments have also demonstrated that bacteriophage-mediated lysis of cobalamin-producing marine bacteria can release cobalamin into the dissolved pool and make it available to cobalamin auxotrophic phytoplankton (Sultana et al., 2025). Although Ado-B_{12} represented a smaller fraction of the dissolved

https://doi.org/10.5194/egusphere-2026-5019
Preprint. Discussion started: 14 September 2026
© Author(s) 2026. CC BY 4.0 License.

cobalamin pool than OH-B_{12}, its occurrence in some intermediate-water samples is noteworthy because this coenzyme form is relatively unstable in seawater (Bannon et al., 2024). Its presence may therefore reflect relatively recent production and/or release of intracellular cobalamin, even though its distribution was not significantly related to AOU. Taken together, the contrasting distributions of OH-B_{12} and Ado-B_{12} suggest that the subsurface dissolved cobalamin pool cannot be explained solely by organic matter remineralization, but likely reflects the balance among microbial production, regeneration, transformation, and utilization.

Microbial community composition provides additional context for this subsurface accumulation. The relative abundance of Nitrosopumiliaceae increased below the SCM and was positively associated with TD-B_{12} concentrations from the surface to the upper NPIW. Previous studies have suggested a connection between ammonia-oxidizing archaea (AOA) and marine cobalamin cycling; for example, elevated particulate corrinoid concentrations have been observed in subsurface waters where AOA are abundant (Heal et al., 2018). Although the observed community composition cannot identify the organisms responsible for cobalamin production or determine the balance between production and utilization, the correspondence observed here is consistent with a possible link between cobalamin accumulation and microbial community composition from the surface to the upper NPIW.

Importantly, the positive relationship between TD-B_{12} and AOU was not maintained in the lower NPIW and deeper waters. AOU remained high, whereas dissolved cobalamin concentrations were variable and frequently lower than those in the upper NPIW. This decoupling indicates that dissolved cobalamin does not accumulate continuously with progressive organic matter remineralization in the same manner as conventional regenerated nutrients. Instead, the balance among microbial production, regeneration, utilization, and removal appears to change with depth, while physical transport may further modify these biological signals, as discussed below.

4.2 Influence of water masses on dissolved cobalamin distributions

In addition to local biological and biogeochemical processes, water-mass transport appears to play an important role in shaping dissolved cobalamin distributions in the western North Pacific. Relatively high TD-B_{12} concentrations extended from below the SCM into the upper NPIW, particularly at stations north of 20°N. The upper NPIW is strongly influenced by waters originating from the Okhotsk Sea, whereas the lower NPIW receives a larger contribution from waters associated with the East Kamchatka Current (Yasuda et al., 2001). Because the NPIW is an important pathway for the transport of regenerated nutrients and trace elements from subpolar and marginal-sea regions into the interior North Pacific (e.g. Nishioka et al., 2021), it may similarly redistribute dissolved cobalamin produced or regenerated in intermediate waters or supplied from the source regions of the upper NPIW, including the Okhotsk Sea.

The association of elevated cobalamin concentrations with the upper NPIW is consistent with the large-scale transport by micronutrients with intermediate waters. For example, dissolved Fe concentrations in the western North Pacific are enhanced within the NPIW through lateral transport from marginal seas and continental margins (Nishioka et al., 2020). An intermediate-water maximum has also been reported for dissolved Co (Zheng et al., 2019; Morton et al., 2019), the central

https://doi.org/10.5194/egusphere-2026-5019
Preprint. Discussion started: 14 September 2026
© Author(s) 2026. CC BY 4.0 License.

metal ion of cobalamin. Cobalt availability may be relevant to cobalamin cycling because Co addition has been shown to enhance cobalamin production by natural microbial communities (Panzeca et al., 2008). Thus, lateral transport of Co-rich intermediate waters could potentially support microbial cobalamin production within the NPIW, in addition to the direct transport of dissolved cobalamin itself. Although dissolved Co concentrations and rates of cobalamin production were not measured in the present study, the elevated TD-B_{12} concentrations in the upper NPIW are consistent with an interplay between local microbial cycling and lateral transport, highlighting the potential role of intermediate waters in shaping dissolved cobalamin distributions.

In deeper waters, TD-B_{12} concentrations were generally lower than those observed in the upper NPIW, although localized increases were observed at several stations, particularly near the bottom at approximately 5,000 m depth. These increases were largely attributable to OH-B_{12}. Stations with elevated cobalamin concentrations in near-bottom waters were located along pathways potentially influenced by UCDW and LCDW (Kawabe and Fujio, 2010). The present observations represent a spatial snapshot and do not distinguish between transport by these water masses and local production or supply. The spatial correspondence suggests a potential contribution of deep circulation to the large-scale distribution of dissolved cobalamin.

Sedimentary input represents another possible source of the elevated cobalamin concentrations observed near the seafloor. Early studies in Japanese coastal waters reported substantially higher cobalamin concentrations in sediments than in overlying bottom waters (Kurata et al., 1970), and high sedimentary cobalamin concentrations have also been reported from the East China Sea and Pacific Ocean (Ohwada and Taga, 1969). These observations suggest that marine sediments may represent an important reservoir of cobalamin. Benthic inputs, followed by redistribution through deep-water circulation, may therefore contribute to the localized bottom-water enrichments observed in this study. Thus, biological processes and water-mass transport jointly shape the vertical and zonal distributions of dissolved cobalamin in the western North Pacific.

5. Conclusions

This study provides one of the few basin-scale observations of multiple dissolved cobalamin species from the surface to the deep ocean. Dissolved cobalamin concentrations were generally low in surface waters but increased below the SCM and within the upper NPIW, where TD-B_{12} and OH-B_{12} were associated with AOU and changes in microbial community composition. In contrast, this relationship weakened in the lower NPIW and deeper waters, while localized increases in OH-B_{12} occurred in some deep and bottom waters. These observations suggest that dissolved cobalamin distributions in the western North Pacific reflect a dynamic balance among microbial production, regeneration, biological utilization, degradation, and physical transport, with the relative importance of these processes changing with depth and water-mass structure.

https://doi.org/10.5194/egusphere-2026-5019
Preprint. Discussion started: 14 September 2026
© Author(s) 2026. CC BY 4.0 License.

Data availability

The 16S rRNA gene amplicon sequence data have been deposited with links to BioProject accession number PRJDB20174 in the DDBJ BioProject database. Other data, including hydrographic data and dissolved cobalamin have been made available in the research data repository of Nagasaki University NAOSITE (http://hdl.handle.net/10069/0002004390). The surface nitrate concentrations data used in Fig. 1 was obtained from https://odv.awi.de/data/ocean/world-ocean-atlas-2018/.

Author contribution

YKondo contributed to the design of the research. YKondo, YKawakami, HO, and JN performed the sampling. YKondo, YKawakami, TT, and TS measured the samples and analyzed the data. YKondo prepared the manuscript with inputs from H O and JN. YKondo, YKawakami, and JN contributed to the funding acquisition.

Competing interests

The authors declare that they have no conflict of interest.

Acknowledgements

We sincerely thank the captain, crew, and scientists on board the R/V *Hakuho Maru* KH-22-7 (GEOTRACES GP22) cruise for their assistance at the sea. This study was supported by the Cooperative Research Program of the Atmosphere and Ocean Research Institute, The University of Tokyo (Research Vessel *Hakuho-maru*, JURCAOSSH22-02). We express our sincere appreciation to Dr. K. Suzuki (Hokkaido University) for his advice on sampling the 16S rRNA gene sequence. We thank Drs. S. Takeda and M. Wada (Nagasaki University) for their helpful discussions in improving this article.

Financial support

This study was supported by PRESTO, the Japan Science and Technology Agency (JPMJPR23G5), the Sasakawa Scientific Research Grant from The Japan Science Society (2022-3023), and Grant-in-Aid for Scientific Research (S) MEXT KAKENHI JP21H05056. The international GEOTRACES Programme is possible in part thanks to the support from the U.S. National Scientific Foundation (OCE-21 40395) to the Scientific Committee on Oceanographic Research (SCOR).

References

Bannon, C. C., Mudge, E. M., and Bertrand, E. M.: Shedding light on cobalamin photodegradation in the ocean, Limnol. Oceanogr. Lett., 9, 135–144, https://doi.org/10.1002/lol2.10371, 2024.

https://doi.org/10.5194/egusphere-2026-5019
Preprint. Discussion started: 14 September 2026
© Author(s) 2026. CC BY 4.0 License.

Bannon, C., White, P. L., Rowland, E., More, K. J., Gleason, A., Roberts, M., Devred, E., Beazley, L., LaRoche, J., and Bertrand, E. M.: Seasonal patterns in B-vitamins and cobalamin co-limitation in the Northwest Atlantic, Limnol. Oceanogr., 70, 3370–3385, https://doi.org/10.1002/lno.70204, 2025.

Bertrand, E. M., Saito, M. A., Rose, J. M., Riesselman, C. R., Lohan, M. C., Noble, A. E., Lee, P. A., and DiTullio, G. R.: Vitamin B_{12} and iron colimitation of phytoplankton growth in the Ross Sea, Limnol. Oceanogr., 52, 1079–1093, https://doi.org/10.4319/lo.2007.52.3.1079, 2007.

Bertrand, E. M., Bannon, C. C., Helliwell, K. E., Kondo, Y., Brisbin, M. M., Tausch, A., and Wienhausen, G.: New views on cobalamin in marine microbial ecosystems, Annual Reviews of Marine Science, accepted.

Bostock, H. C., Opdyke, B. N., and Williams, M. J. M.: Characterising the intermediate depth waters of the Pacific Ocean using δ13C and other geochemical tracers, Deep-Sea Res. Pt. I, 57, 847–859, https://doi.org/10.1016/j.dsr.2010.04.005, 2010.

Carlucci, A. F., and Cuhel, R. L.: Vitamins in the South Polar Seas: distribution and significance of dissolved and particulate vitamin B_{12}, thiamine, and biotin in the Southern Indian Ocean, in: Adaptation within Antarctic ecosystems, edited by: Llano, G. A.: Smithsonian Institute, Washington, DC, 115–128, 1977.

Croft, M. T., Lawrence, A. D., Raux-Deery, E., Warren, M. J., and Smith, A. G.: Algae acquire vitamin B_{12} through a symbiotic relationship with bacteria, Nature, 438, 90–93, https://doi.org/10.1038/nature04056, 2005.

Daisley, K. W., and Fisher, L. R.: Vertical distribution of vitamin B_{12} in the sea, J. Mar. Biol. Ass. U. K., 37, 683-686, 1958.

Edler, L. and Elbrächter, M.: The Utermöhl method for quantitative phytoplankton analysis, in: Microscopic and Molecular Methods for Quantitative Phytoplankton Analysis, edited by: Karlson, B., Cusack, C., and Bresnan, E., UNESCO, Paris, 13–20, 2010.

Heal, K. R., Carlson, L. T., Devol, A. H., Armbrust, E. V., Moffett, J. W., Stahl, D. A., and Ingalls, A. E.: Determination of four forms of vitamin B_{12} and other B vitamins in seawater by liquid chromatography/tandem mass spectrometry, Rapid Commun. Mass Sp., 28, 2398–2404, https://doi.org/10.1002/rcm.7040, 2014.

https://doi.org/10.5194/egusphere-2026-5019
Preprint. Discussion started: 14 September 2026
© Author(s) 2026. CC BY 4.0 License.

Heal, K. R., Qin, W., Amin, S. A., Devol, A. H., Moffett, J. W., Armbrust, E. V., Stahl, D. A., and Ingalls, A. E.: Accumulation of NO_2 -cobalamin in nutrient-stressed ammonia-oxidizing archaea and in the oxygen deficient zone of the eastern tropical North Pacific. Environ Microbiol Rep. https://doi.org/10.1111/1758-2229.12664, 2018.

Helliwell, K. E., Lawrence, A. D., Holzer, A., Kudahl, U. J., Sasso, S., Kräutler, B., Scanlan, D. J., Warren, M. J., and Smith, A. G.: Cyanobacteria and eukaryotic algae use different chemical variants of vitamin B_{12}, Curr. Biol., 26, 999–1008, https://doi.org/10.1016/j.cub.2016.02.041, 2016.

Karl, D. M.: Nutrient dynamics in the deep blue sea, Trends in Micobiol., 10, 410-418, https://doi.org/10.1016/S0966-842X(02)02430-7, 2002.

Kawabe, M. and Fujio, S.: Pacific Ocean circulation based on observation, J. Oceanogr., 66, 389–403, https://doi.org/10.1007/s10872-010-0034-8, 2010.

Kurata, A.: Vitamin B_{12} transudation from marine bottom muds, J. Oceanogr. Soc. Jpn., 26, 81–86, 1970.

Menzel, D. W. and Spaeth, J. P.: Occurrence of vitamin B_{12} in the Sargasso Sea, Limnol. Oceanogr., 7, 151–154, 1962.

Morton, P. L., Landing, W. M., Shiller, A. M., Moody, A., Kelly, T. D., Bizimis, M., Donat, J. R., De Carlo, E. H., and Shacat, J.: Shelf inputs and lateral transport of Mn, Co, and Ce in the western North Pacific Ocean, Front. Mar. Sci., 6, 591, https://doi.org/10.3389/fmars.2019.00591, 2019.

Nishioka, J., Obata, H., Ogawa, H., Ono, K., Yamashita, Y., Lee, K., Takeda, S., and Yasuda, I.: Subpolar marginal seas fuel the North Pacific through the intermediate water at the termination of the global ocean circulation, P. Natl. Acad. Sci. USA, 117, 12665–12673, https://doi.org/10.1073/pnas.2000658117, 2020.

Nishioka, J., Obata, H., Hirawake, T., Kondo, Y., Yamashita, Y., Misumi, K., and Yasuda, I.: A review: iron and nutrient supply in the subarctic Pacific and its impact on phytoplankton production, J. Oceanogr., 77, 561–587, https://doi.org/10.1007/s10872-021-00606-5, 2021.

Ohwada, K., and Taga, N.: Distribution of vitamin B12, thiamine and biotin in marine sediments, J. Oceanogr. 25, 123-136, 1969.

https://doi.org/10.5194/egusphere-2026-5019
Preprint. Discussion started: 14 September 2026
© Author(s) 2026. CC BY 4.0 License.

Panzeca, C., Beck, A. J., Leblanc, K., Taylor, G. T., Hutchins, D. A., and Sañudo-Wilhelmy, S. A.: Potential cobalt limitation of vitamin B_{12} synthesis in the North Atlantic Ocean, Global Biogeochem. Cy., 22, GB2029, https://doi.org/10.1029/2007GB003124, 2008.

Parada, A. E., Needham, D. M., and Fuhrman, J. A.: Every base matters: assessing small subunit rRNA primers for marine microbiomes with mock communities, time series and global field samples, Environ. Microbiol., 18, 1403–1414, https://doi.org/10.1111/1462-2920.13023, 2016.

Sañudo-Wilhelmy, S. A., Cutter, L. S., Durazo, R., Smail, E. A., Gómez-Consarnau, L., Webb, E. A., Prokopenko, M. G., Berelson, W. M., and Karl, D. M.: Multiple B-vitamin depletion in large areas of the coastal ocean, P. Natl. Acad. Sci. USA, 109, 14041–14045, https://doi.org/10.1073/pnas.1208755109, 2012.

Sañudo-Wilhelmy, S. A., Gómez-Consarnau, L., Suffridge, C., and Webb, E. A.: The role of B vitamins in marine biogeochemistry, Annu. Rev. Mar. Sci., 6, 339–367, https://doi.org/10.1146/annurev-marine-120710-100912, 2014.

Suffridge, C., Cutter, L., and Sañudo-Wilhelmy, S. A.: A new analytical method for direct measurement of particulate and dissolved B-vitamins and their congeners in seawater, Front. Mar. Sci., 4, 11, https://doi.org/10.3389/fmars.2017.00011, 2017.

Suffridge, C. P., Gómez-Consarnau, L., Monteverde, D. R., Cutter, L., Arístegui, J., Alvarez-Salgado, X. A., Gasol, J. M., and Sañudo-Wilhelmy, S. A.: B vitamins and their congeners as potential drivers of microbial community composition in an oligotrophic marine ecosystem, J. Geophys. Res.-Biogeo., 123, 2890–2907, https://doi.org/10.1029/2018JG004554, 2018.

Sultana, S., Bruns, S., Pacheco-Valenciana, A., Mehrshad, M., Wilkes, H., Simon, M., Garcia, S., and Wienhausen, G.: Vitamin B_{12} release through bacteriophage-mediated cell lysis of the marine bacterium *Sulfitobacter* sp. M39, ISME Commun., 5, ycaf136, https://doi.org/10.1093/ismeco/ycaf136, 2025.

Talley, L. D., Pickard, G. L., Emery, W. J., and Swift, J. H.: Descriptive Physical Oceanography: An Introduction, 6th Edn., Academic Press, 2011.

Welschmeyer, N. A.: Fluorometric analysis of chlorophyll a in the presence of chlorophyll b and pheopigments, Limnol. Oceanogr., 39, 1985–1992, https://doi.org/10.4319/lo.1994.39.8.1985, 1994.

https://doi.org/10.5194/egusphere-2026-5019
Preprint. Discussion started: 14 September 2026
© Author(s) 2026. CC BY 4.0 License.

Yasuda, I., Okuda, K., and Shimizu, Y.: Hydrographic structure and transport of the Oyashio south of Hokkaido and the formation of North Pacific Intermediate Water, J. Geophys. Res.-Oceans, 106, 6931–6942, https://doi.org/10.1029/1999JC000154, 2001.

Yasuda, I.: Hydrographic structure and variability in the Kuroshio–Oyashio transition area, J. Oceanogr., 59, 389–402, https://doi.org/10.1023/A:1025580313836, 2003.

Zheng, L., Minami, T., Konagaya, W., Chan, C.-Y., Tsujisaka, M., Takano, S., Norisuye, K., and Sohrin, Y.: Distinct basin-scale distributions of aluminum, manganese, cobalt, and lead in the North Pacific Ocean, Geochim. Cosmochim. Ac., 254, 102–121, https://doi.org/10.1016/j.gca.2019.03.038, 2019.